Zhang *et al. Biochar* (2026) 8:48
https://doi.org/10.1007/s42773-025-00567-8

Biochar

ORIGINAL RESEARCH Open Access

Novel multi-interface regulation of acetochlor fate in a soil-plant system using N-doped biochar-modified zero-valent iron nanocomposites for enhanced degradation and protective root iron plaque formation

Xiangyu Zhang[1], Peng Zhang[2*], Le Jiao[3], Yanwei Zhang[3], Hongwen Sun[2] and Chenglan Liu[1*]

Abstract

Agricultural herbicide contamination in soil poses a significant challenge to global food security and ecosystem health. However, conventional remediation strategies often neglect the co-control of parent compounds and their more mobile transformation products, thereby increasing the risks of crop uptake and incomplete detoxification. Here, we have developed a novel nitrogen-doped biochar-modified zero-valent iron nanocomposite (NC-ZVI) that enables multi-interface regulation of pollutants in soil–plant systems, simultaneously promoting soil remediation and safeguarding crop health. Engineering of atomic Fe–C and Fe–N coordination along with N-doped active sites modulated the electronic structure of ZVI, enhancing the surface reactivity and electron capability in NC-ZVI. This enabled rapid removal of approximately 90% of acetochlor in soil within 7 d by reinforced interfacial catalytic degradation. NC-ZVI also promoted the release of iron ions, driving the formation of iron plaques on maize root surfaces. These plaques established a dynamic protective barrier that reduced the total concentrations of acetochlor and its degradation products in maize by 81.2% while maintaining iron nutrient uptake. The multi-interface interaction strategy not only restored maize productivity, increasing its aboveground biomass by 208.4%, but also preserved soil microbial diversity, all at a cost-competitive level. Overall, this work advances the understanding of the interactions between biochar-based materials and pollutants in soil–plant systems, providing a powerful tool to tackle soil pollution and enhance food safety.

Highlights

- NC-ZVI enables multi-interface regulation for acetochlor remediation in soil–plant systems.
- Approximately 90% acetochlor removal in soil was achieved via enhanced catalytic degradation.
- Root iron plaque reduces maize uptake of acetochlor and its byproducts by 81.2%.
- The strategy promotes maize growth and preserves soil microbial diversity.

Keywords Nano remediation, Biochar, Zero-valent iron, Catalytic degradation, Iron plaque, Food safety

*Correspondence:
Peng Zhang
nkzhangpeng@nankai.edu.cn
Chenglan Liu
liuchenglan@scau.edu.cn
Full list of author information is available at the end of the article

Springer

Graphical Abstract

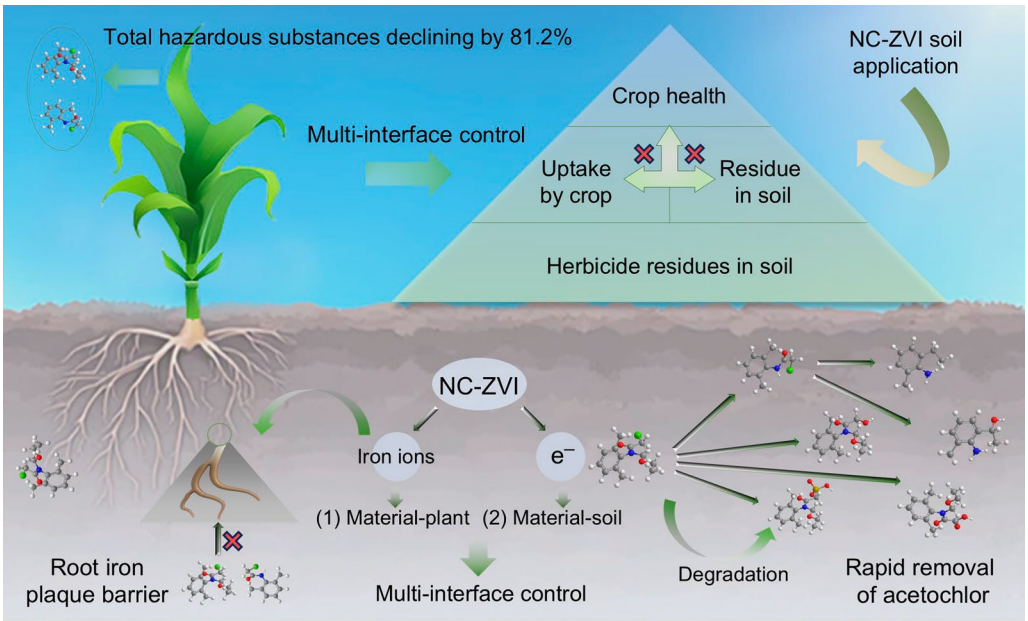

1 Introduction

The escalating global population and rising food demand pose severe challenges to agricultural systems (Herrick et al. 2024). These challenges are exacerbated by widespread soil contamination caused by agricultural chemicals, including pesticides and antibiotics, among others (Tang et al. 2021; Li et al. 2025; Zhao et al. 2025). According to the United Nations Food and Agriculture Organization (FAO), pesticide pollution results in annual economic losses exceeding billions of dollars and reduces global crop yields by millions of metric tons (Food and Agriculture Organization of the United Nations. 2015; Leng et al. 2023). Among them, the chloroacetamide herbicide acetochlor warrants particular attention due to its widespread use, with annual application exceeding 10,000 tons in China alone, and its frequent detection in soil and water systems, driven by its high environmental persistence. More critically, acetochlor is classified as a B-2 carcinogen by the U.S. Environmental Protection Agency and exhibits pronounced phytotoxicity to subsequent crops, representing a dual threat to ecosystem stability and food safety (Li et al. 2018; Guan et al. 2020; Hoang et al. 2021). Therefore, it is urgent to develop efficient in situ remediation technologies for such contaminants.

Zero-valent iron (ZVI) exhibits great potential in environmental remediation due to its strong reduction activity and catalytic capacity (Liu et al. 2021, 2022; Xu et al. 2024). However, its intrinsic limitations, including rapid surface oxidative passivation, particle aggregation, and inefficient electron transfer to organic pollutants adsorbed by soil, severely limit its agricultural application (Li et al. 2021b; Qu et al. 2023; Xie et al. 2024). More importantly, agricultural remediation scenarios impose stringent time constraints. The brief intervals between crop rotations necessitate that remediation technologies simultaneously achieve rapid pollutant degradation and crop protection within extremely limited timeframes (Zeller et al. 2021; Xie et al. 2023), placing far greater demands on the efficiency of ZVI-based materials compared to industrial site remediation. Furthermore, ZVI-based technologies often fail to achieve complete mineralization of organic pollutants, leading to the generation of numerous water-soluble degradation products. These intermediates are more mobile in the soil matrix and can be readily absorbed by plants, potentially causing secondary contamination within the soil–plant system (Huang et al. 2022; Gong et al. 2025; Han et al. 2025). Hence, achieving efficient co-management of parent pollutants and their transformation products under real-world agricultural constraints remains a core challenge that must be addressed before ZVI technology can be successfully deployed in the field.

Recent advances in non-metal doping (e.g., S, P, N) have established effective pathways to enhance ZVI reactivity by mitigating passivation and facilitating electron transfer (Gong et al. 2021; Chen et al. 2024; Wang et al. 2025). Unlike sulfidation, which primarily improves electron transfer, or phosphatization, which enhances surface stability, concurrent N and C co-doping (N/C-doping) offers a more integrated approach by reconstructing the atomic coordination environment of iron. Within the resulting Fe–N–C structures, Fe–N sites optimize the coordination environment around iron atoms, thereby lowering the energy barrier for contaminant reduction and promoting sustained Fe(II) release (Gong et al. 2021; Li et al. 2023). This structure-specific design not only enhances interfacial electron transfer for catalytic degradation of pollutants but also strengthens the hydrophobicity required for efficient pollutant capture from soil matrices, offering a structurally distinct and mechanistically superior alternative to existing modified ZVI materials. However, research on applying such materials in soil remediation remains relatively limited. Furthermore, emerging evidence indicates that under abiotic stress conditions, plant roots can secrete acidic substances that synergistically regulate rhizosphere iron dynamics with iron oxides (e.g., α-Fe_2O_3), promoting the formation of protective iron plaque (Zheng et al. 2024). This phenomenon, which has been extensively documented in wetland plants through radial oxygen loss (Wang et al. 2021a; Wei et al. 2022b; Meng et al. 2024), can now be effectively induced in upland by leveraging highly reactive iron-based material systems that regulate Fe(II)/Fe(III) cycling and promote iron dissolution. This novel strategy could simultaneously reduce pollutant concentration and bioavailability while maintaining essential iron nutrition for crops. However, the activity of ZVI, particularly multifunctional non-metal atom-doped ZVI materials, and their efficacy in inhibiting crop uptake of contaminants and their transformation products by promoting iron plaque formation within agricultural systems, remain unexplored.

Based on these insights, we have developed a novel N/C-doped ZVI nanomaterial (NC-ZVI) to establish a "soil catalytic degradation-root iron plaque barrier" strategy for contaminated soil–plant systems (Fig. 1a), aiming to simultaneously achieve efficient soil remediation and ensure crop health. Given that maize (*Zea mays L.*), a dryland crop, is of great significance in global agriculture and has widespread exposure to acetochlor contamination, it was selected as the model crop for this work (Yan et al. 2023). The specific objectives were to (1) synthesize and characterize the NC-ZVI and evaluate its efficacy in enhancing acetochlor degradation and reducing the accumulation of its parent molecules and degradation products in maize; (2) elucidate the dual mechanisms of catalytic degradation in soil and iron plaque-mediated barrier formation on root surfaces in contaminated soil–plant systems; (3) assess the practical potential of NC-ZVI by investigating its ecological compatibility with soil microbiota and performing a preliminary techno-economic analysis to gauge its field application feasibility. These findings transcend conventional nano-remediation by integrating material innovation with soil–plant feedback, thereby advancing sustainable development strategies for global eco-environmental protection and safe crop production.

2 Materials and methods

2.1 Sample preparation

Technical-grade acetochlor (99.0% purity) and its primary degradation products (acetochlor OXA, acetochlor ESA, acetochlor 2-OH, (2-chloro-N-(2-ethyl-6-methyl phenyl) acetamide (CMEPA), 2-ethyl-6-methylaniline (EMA), and 2-(1-hydroxyethyl)-6-methylaniline (HEMA)) were obtained from Tianjin Alta Technology Co., Ltd. (China). The physicochemical properties of these compounds are summarized in Table S1. Maize seeds (*Zea mays L.* cv. Jinyinsu 2) were provided by the Maize Research Institute of the Guangdong Academy of Agricultural Sciences. Soil samples were collected from a maize field in Guangdong, China, which is classified as sandy loam with a pH of 5.51 ± 0.02. NC-ZVI and S-ZVI were synthesized via mechanochemical ball milling according to a previously reported method (Text S1) (Gu et al. 2017; Li et al. 2023). Commercial nZVI and mZVI were purchased from Aladdin Biochemical Technology Co., Ltd. (China). A detailed characterization of nZVI, mZVI, NC-ZVI, and S-ZVI is described in Text S2.

2.2 Pot experiments

A predetermined amount of air-dried soil was uniformly mixed with an acetone-based acetochlor stock solution and subsequently placed in a fume hood to allow for complete acetone evaporation. The resulting mixture was then progressively diluted with fresh soil at a mass ratio of 1:10 to achieve the target acetochlor concentration of 5.0 mg kg^{-1}, as established based on residue levels reported in a previous study (Arshad et al. 2024). Subsequently, NC-ZVI (1.0 g kg^{-1}, optimized through pre-experiments shown in Fig. S1) was incorporated into the acetochlor-contaminated soil. Each pot contained 500 g of soil sample, to which deionized water was added to achieve a soil moisture content of 60% of its maximum water-holding capacity. After equilibration for 24 h, three healthy maize seeds were randomly sown into the prepared soil and transferred to a greenhouse at 25 ± 5 °C. Each treatment was watered daily to ensure adequate

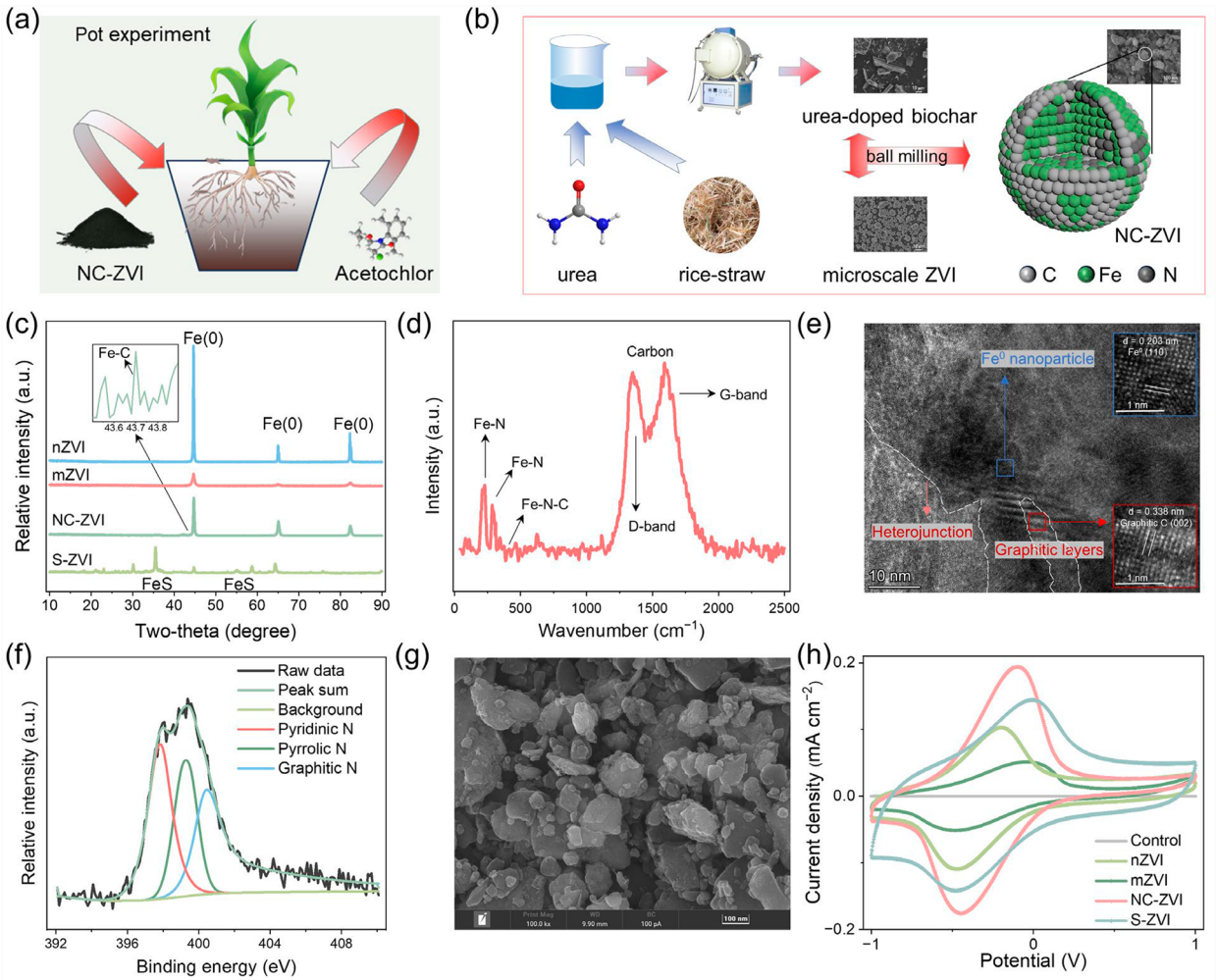

Fig. 1 Mechanochemical synthesis and structural features of NC-ZVI. **a** Schematic of the pot experiment setup. **b** Schematic diagram of NC-ZVI synthesized by mechanochemical ball milling. **c** XRD patterns of nZVI, mZVI, NC-ZVI, and S-ZVI. **d** Raman spectra of NC-ZVI. **e** TEM image of NC-ZVI. **f** XPS spectra of N 1 s for the NC-ZVI particles, and the fitted peaks correspond to pyridinic N, pyrrolic N, and graphitic N. **g** SEM image of NC-ZVI. **h** CV curves of nZVI, mZVI, NC-ZVI, and S-ZVI

soil moisture levels. All treatments were conducted with three independent biological replicates (n = 3), with each replicate consisting of three maize plants in the same pot. Additionally, a blank control group without acetochlor under maize planting conditions and another treatment group containing both acetochlor and ZVI materials without maize cultivation were established.

2.3 Plant harvesting and determination of growth parameters

On day 21 post-sowing, the maize plants were harvested and rinsed three times with deionized water. For each pot, the three plants were pooled together to form a composite sample as one biological replicate for analysis, and the fresh biomass of root and leaf was immediately recorded. Leaf chlorophyll content was quantified using spectrophotometry as described in Text S3 (Zhang et al. 2023). Oxidative damage to leaves was evaluated through fluorescence analysis and spectrophotometry (Text S4) (Radwan. 2012). The total iron content in the maize plants was determined via flame atomic absorption spectroscopy after acid digestion with $HNO_3/HClO_4/H_2O_2$ (5:2:1) (Text S5) (Grillet et al. 2018).

2.4 Determination of acetochlor in soil and plant tissues

Freeze-dried soil (5 g) and plant tissues (0.5 g) were extracted using the improved QuEChERS method (González-Curbelo et al. 2015), and the concentrations of acetochlor and its degradation products (acetochlor OXA, acetochlor ESA, acetochlor 2-OH, CMEPA, EMA,

and HEMA) were quantified via ultrahigh-performance liquid chromatography (UPLC-MS/MS), as detailed in Text S6. A standard curve (0.01–5.0 mg kg^{-1}) and spiked matrix were used to verify the recovery rates of acetochlor and its degradation products in both soil and maize tissues (79.4–110.4%; Table S2). Moreover, the toxicity of the products to non-target organisms (e.g., green algae, daphnia, fish) was speculated using the Ecological Structure Activity Relationships (ECOSAR) predictive model (Reuschenbach et al. 2008).

2.5 Desorption-enhanced degradation of acetochlor mediated by NC-ZVI in soil

The desorption-enhanced chemical degradation mechanism of acetochlor mediated by NC-ZVI was systematically evaluated through amphiphilicity characterization, aqueous-phase adsorption experiments, and soil-phase desorption tests (Text S7) (Wang et al. 2024). To quantify the microbial contributions to acetochlor degradation, degradation experiments were conducted in both sterilized and unsterilized soils to examine the impact of soil microorganisms on acetochlor degradation, following the methodologies specified in Text S8 (Liu et al. 2021).

2.6 Iron plaque characterization and its role in preventing plant uptake of pollutants

The maize root surface was analyzed with the scanning electron microscopy coupled with energy dispersive spectroscopy (SEM–EDS, Hitachi Regulus 8100), and cross-sections of the roots were examined via a biological transmission electron microscope (TEM) equipped with EDS (Hitachi 7800). The detailed procedures are described in Text S9. Moreover, iron plaque was extracted from the roots using a dithionite-citrate-bicarbonate (DCB) solution (Amaral et al. 2017), and the concentrations of acetochlor and its degradation products in the iron plaque were quantified (Text S10). To investigate the mechanism of iron plaque formation and its role in inhibiting maize acetochlor uptake, organic acid content in root exudates was measured (Text S11); simultaneously, maize plants were cocultured with ZVI materials for 21 d prior to transplantation into acetochlor-contaminated soil, after which the acetochlor concentration in the leaf tissues was measured.

2.7 Soil microbial community analysis

Microbial DNA was extracted from the soil samples via a soil DNA Kit (Omega Biotek), and the operation protocol is detailed in Text S12 (Bokulich et al. 2013; Wang et al. 2021b). The raw files for the DNA sequence extracted from soil samples can be obtained from the NCBI Sequence Read Archive (SRA) platform via ID PRJNA1193536, and the raw data were processed through splicing and filtering to yield valid data. These validated datasets were subsequently analyzed by Novogene Bioinformatics Technology Co. Ltd using the QIIME2 platform via the DADA2 algorithm, which excluded sequences with abundances of less than 5, and the amplicon sequence variants (ASVs) were obtained. Taxonomic assignment of ASVs was performed against the SILVA 138.1 database. The soil microbial α-diversity was assessed via the Chao1, Shannon, and Simpson indices, whereas the principal coordinate analysis (PCoA) was used to assess β-diversity. SIMPER analysis was performed via PRIMER-e v7 software (the similarity threshold set at 70%) to identify key phylum contributing to variations in bacterial community structure between paired treatments.

2.8 Statistical analysis

The data were analyzed using IBM SPSS 26.0 software, and the descriptive statistics are shown as averages and standard deviations (mean ± s.d.). A two-tailed unpaired t-test was employed at a 95% confidence level to compare the mean ± s.d. of two independent groups. To compare the mean ± s.d. of a single variable across three or more independent groups, the one-way analysis of variance (ANOVA) followed by Tukey's post hoc tests was applied. The significant difference was represented by the p value.

3 Results and discussion

3.1 Characterization of NC-ZVI

NC-ZVI was successfully synthesized through a ligand-assisted mechanochemical approach involving high-energy ball milling of micron-sized ZVI powder with urea-doped biochar (NBC) (Fig. 1b). This process enabled atomic-level N/C doping into the ZVI lattice and established strong interfacial interactions between ZVI and NBC. X-ray diffraction (XRD) and Raman spectra confirmed the formation of Fe–C and Fe–N coordination bonds in NC-ZVI (Fig. 1c, d) (Gao et al. 2015; Gong et al. 2021), with TEM analysis providing direct evidence of these atomic-scale interactions (Fig. 1e). Furthermore, X-ray photoelectron spectroscopy (XPS) analysis of the N 1 s spectrum revealed three characteristic peaks at 398.4, 399.6, and 401.1 eV (Fig. 1f), corresponding to pyridinic N, pyrrolic N, and graphitic N species, respectively (Huang et al. 2022). These nitrogen configurations synergistically enhanced the redox reactivity of NC-ZVI. Specifically, graphitic N facilitated electron transfer through N–C–Fe-driven redox reactions, while pyridinic/pyrrolic N coordinated with Fe atoms through lone-pair electron donation, collectively optimizing the adsorption and degradation capacity of NC-ZVI for reactants (Lin et al. 2014; Chen et al. 2017).

SEM images revealed a homogeneous dispersion of NC-ZVI particles with a diameter of approximately 100 nm (Fig. 1g), which is in sharp contrast to the significant agglomeration and oxidative morphology observed for S-ZVI and nZVI (Fig. S2). The specific surface area (SSA) of NC-ZVI was measured at 18.12 $m^2 g^{-1}$ (Table S3), representing a 6.6-fold increase compared to unmilled ZVI (2.74 $m^2 g^{-1}$). This enhanced SSA provides more active sites for pollutant adsorption and degradation. Electrochemical characterization confirmed the modulating effect of N/C doping on the electronic structure. Cyclic voltammetry (CV) curves showed that both NC-ZVI and S-ZVI exhibited significantly increased current densities and redox peaks (Fig. 1h), indicating the facilitative role of N/C and S coordination atoms in promoting electron transfer and redox reactions. Notably, NC-ZVI outperformed S-ZVI in terms of potential difference and cyclic reversibility, which can be attributed to the N-doped active sites and alloying heterojunctions nanoarchitectures formed on NC-ZVI. Correspondingly, the i-t curve provided evidence of electron transfer between NC-ZVI and acetochlor. The free corrosion potentials of NC-ZVI and nZVI were determined to be −769 and −494 mV, respectively, with the decrease in this potential being associated with an increase in charge transfer resistance (Fig. S3). Collectively, these results indicate that the N/C-coordination induces the formation of a ZVI nanoarchitecture, which may exhibit enhanced catalytic degradation activity toward target pollutants.

3.2 NC-ZVI mediated maize physiological responses and soil acetochlor detoxification

The effects of NC-ZVI, S-ZVI, mZVI, and nZVI at a dosage of 1.0 g per kg soil on maize growth in acetochlor-contaminated soil after 21 d are presented in Fig. 2a. The average fresh biomass of maize plants in the control group without acetochlor exposure was 10.1 g (Fig. 2b). Exposure to acetochlor resulted in a significant 67.9%

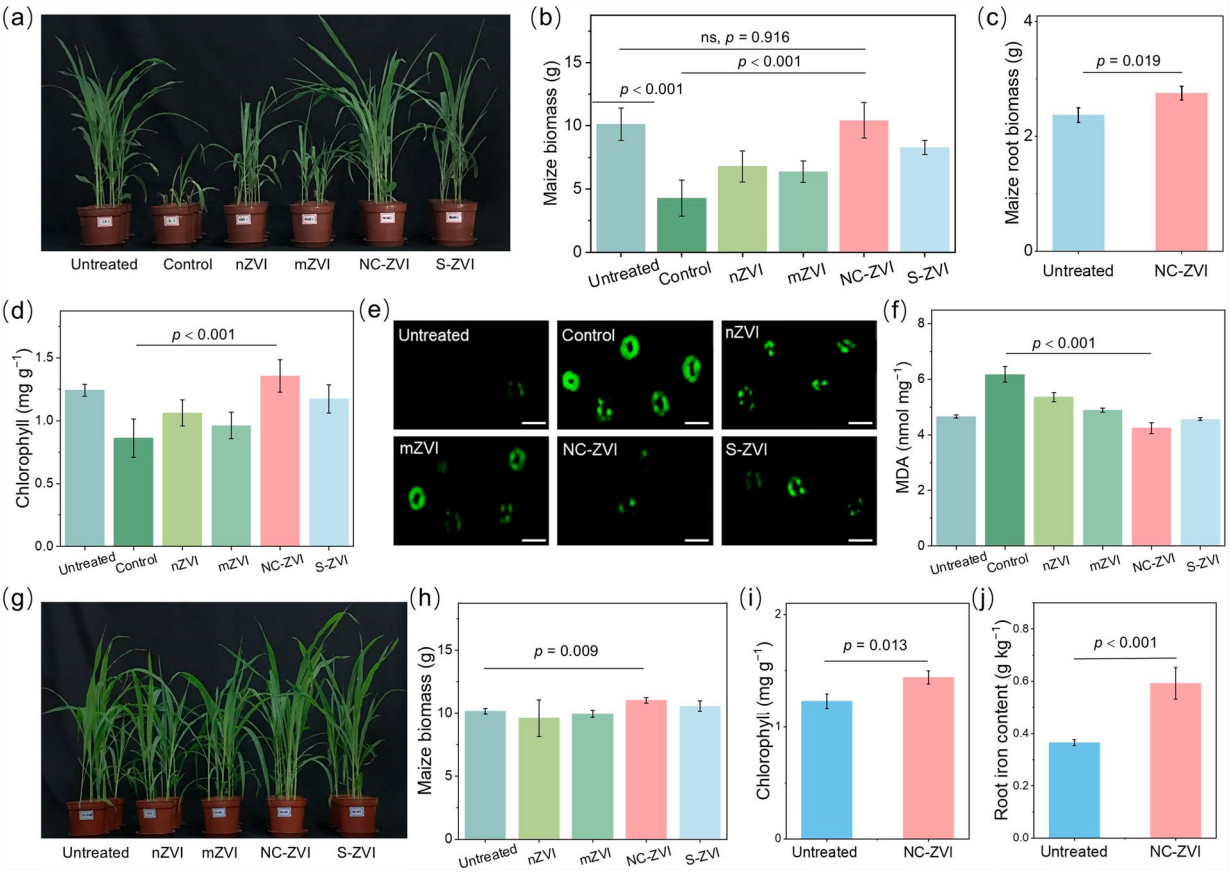

Fig. 2 NC-ZVI enhances maize growth and mitigates acetochlor toxicity. **a** Photographs of maize plants treated with uncontaminated soil (Untreated), acetochlor-contaminated soil (Control), and acetochlor-contaminated soil amended with nZVI, mZVI, NC-ZVI, and S-ZVI (left to right). **b** Fresh maize biomass, **c** fresh root biomass, **d** chlorophyll content, **e** ROS fluorescence images (the deeper the color, the higher the ROS content, scale bar = 50 μm), and (**f**) MDA enzyme activity across all treatments. **g** Photographs of the maize plants and **h** maize biomass in ZVI-amended uncontaminated soil. **i** Chlorophyll content and **j** root iron content under NC-ZVI treatment. ns is not significant

reduction in maize biomass compared to the control group. Notably, the application of NC-ZVI reversed this growth suppression and enhanced maize aboveground biomass by 208.4% relative to the acetochlor-contaminated group. Furthermore, compared with the control group without acetochlor, NC-ZVI increased the root biomass by 16.2% (Fig. 2c). Meanwhile, acetochlor exposure impaired maize photosynthetic capacity, reducing total chlorophyll content by 30.7% relative to the control group without acetochlor (Fig. 2d). NC-ZVI treatment restored chlorophyll synthesis, increasing the chlorophyll content by more than 36.1%, whereas nZVI and mZVI showed negligible effects. This recovery in photosynthetic capacity correlated with attenuated oxidative damage (Fig. 2e), as evidenced by a 31.3% reduction in malondialdehyde (MDA) levels in maize compared to the acetochlor-exposed group (Fig. 2f). Concurrent activation of the antioxidant defense system was observed, with total phenolic content and antioxidant capacity increasing by 118.1% and 33.1%, respectively (Fig. S4). These findings indicate that NC-ZVI exerts significant protective effects against acetochlor-induced stress and promotes maize growth. The dual growth-promoting effect of NC-ZVI surpasses that of S-ZVI, nZVI, and mZVI, which can be attributed to its high reactivity with acetochlor and enhanced iron bioavailability mediated by improved interfacial interactions between maize roots and NC-ZVI (Liu et al. 2021). Similar effects were observed when NC-ZVI was applied alone in soil without acetochlor, which significantly increased maize plant biomass and root iron content (Fig. 2g–j).

The soil detoxification efficacy of acetochlor was quantified through the distribution analysis of acetochlor and its primary degradation products (e.g., acetochlor OXA and acetochlor ESA) in maize roots and leaves. In the acetochlor alone-contaminated control, 80.6% of detected residues remained as parent acetochlor (0.41 mg kg^{-1}), indicating limited degradation (Fig. 3a). NC-ZVI amendment significantly reduced root acetochlor accumulation by 80.1%, surpassing the performance of S-ZVI (71.0%), nZVI (26.2%), and mZVI (13.7%). Additionally, NC-ZVI effectively restricted acropetal translocation, decreasing leaf residues by 91.8% compared to 13.8–67.7% achieved by other ZVI materials. Crucially, NC-ZVI demonstrated exceptional metabolic interception

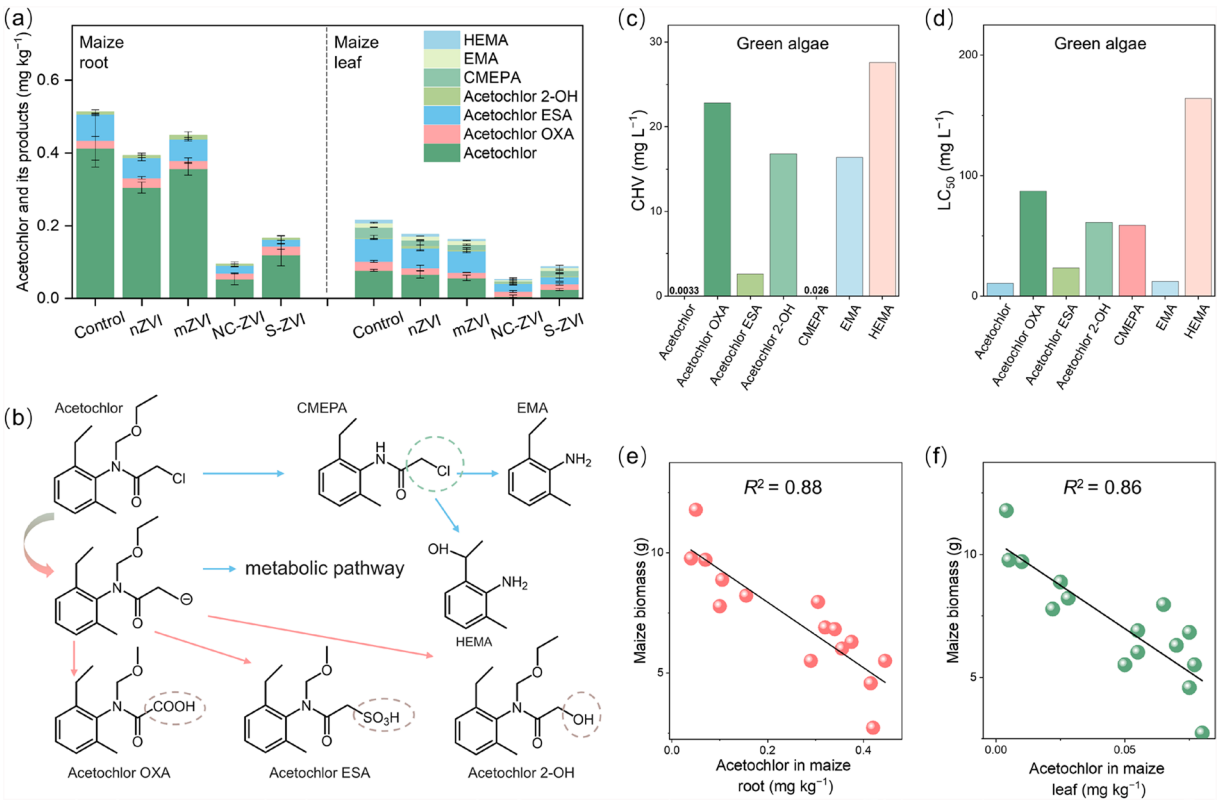

Fig. 3 NC-ZVI modulates acetochlor fate in soil-maize systems. **a** Contents of acetochlor and its degradation products in maize roots and leaves. **b** Proposed degradation pathway of acetochlor in soil-maize systems. **c** Chronic toxicity and **d** acute toxicity of acetochlor and its byproducts to green algae. Correlation analysis between fresh maize biomass and acetochlor residues in maize (**e**) root and (**f**) leaf (n = 15)

capacity and barrier effects against pollutant transfer. Specifically, the persistent metabolite of acetochlor, CMEPA (2-chloro-N-(2-ethyl-6-methyl phenyl) acetamide), constituted 11.5% of leaf residues in the acetochlor-contaminated control, with its proportion decreasing by 96.8% in the NC-ZVI treatment. Toxicity simulations confirmed that CMEPA poses comparable phytotoxic and human health risks to parent acetochlor (Fig. 3b–d; Fig. S5), consistent with previous reports by Wang et al., which indicated that CMEPA induces apoptosis and poses toxicity risks (Wang et al. 2023). Moreover, multivariate regression analysis revealed a significant negative correlation ($R^2 = 0.77–0.91$) between maize biomass and the detected concentrations of acetochlor and its degradation products in maize roots and leaves (Fig. 3e, f; Fig. S6). Therefore, it is reasonable to conclude that NC-ZVI effectively mitigates the accumulation of both acetochlor and its degradation products in maize plants, establishing its dual-action remediation mechanism in the soil–plant system: (1) degradation of acetochlor in soil and (2) iron plaque-mediated barrier blocking root-to-leaf transport of acetochlor and its degradation products (discussed below).

3.3 Degradation of acetochlor in NC-ZVI-amended soil

The catalytic performance of NC-ZVI for acetochlor degradation in maize-cultivated soil systems was systematically evaluated in both planted and unplanted soil systems. As shown in Fig. 4a, b, NC-ZVI achieved 90.7% acetochlor removal within 7 d under maize cultivation, increasing to 96.7% by day 21, whereas the natural attenuation rate was only 32.5% within 21 d for the acetochlor-contaminated group. Similarly, significant differences were also observed in the degradation rates of four types of ZVI materials over 21 d in uncultivated soils, ranked in descending order as follows: NC-ZVI (88.9%) > S-ZVI (75.0%) > nZVI (42.6%) > mZVI (30.7%) (Fig. S7), with consistent trends also noted in aquatic degradation experiments (Fig. S8). These findings demonstrate the superior catalytic degradation capability of NC-ZVI for rapid soil detoxification, which can be attributed to its strong electron-donating capacity toward acetochlor, as confirmed by comprehensive characterization and electrochemical analysis of NC-ZVI.

In general, hydrophobic organic pollutants are easily adsorbed and retained in soil particles, limiting their mass transfer and thereby reducing the catalytic performance of remediation materials toward pollutants (Umeh et al. 2017). In this study, the amphiphilic properties of NC-ZVI and its influence on acetochlor

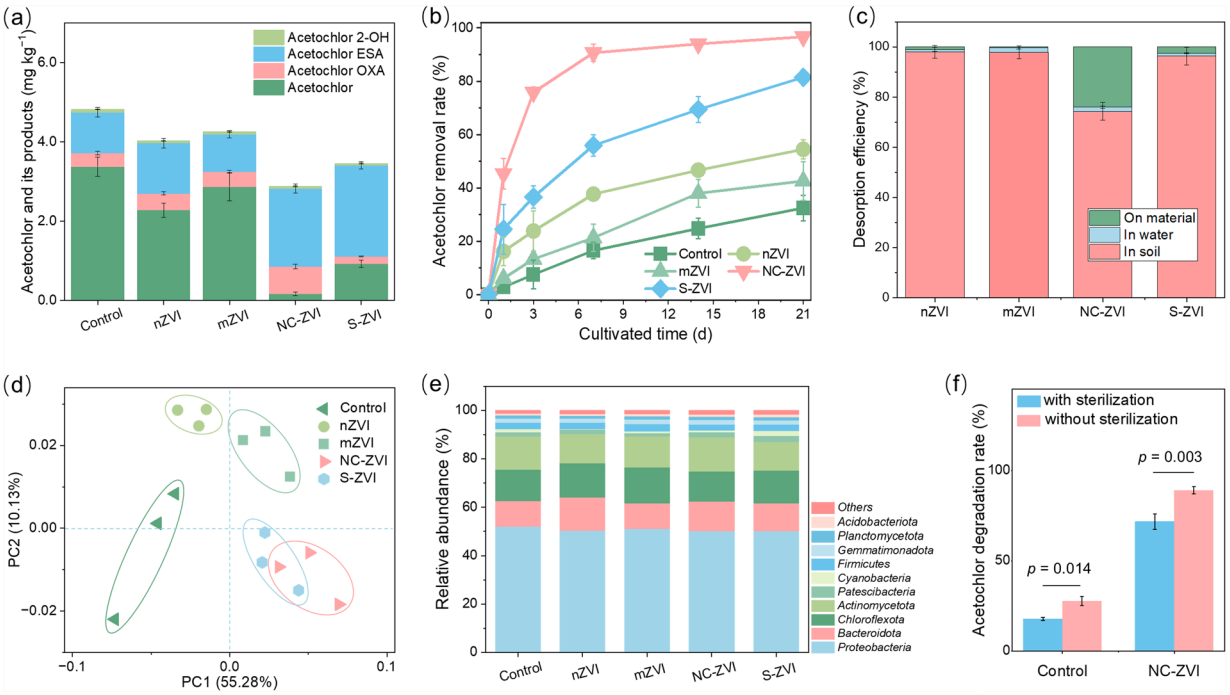

Fig. 4 Degradation dynamics of acetochlor in soil treated with NC-ZVI. **a** Contents of acetochlor and its degradation products in maize-cultivated soil. **b** Acetochlor removal rate in maize-cultivated soil. **c** Desorption efficiency of soil phase-acetochlor for NC-ZVI. **d** PCoA analysis of microbial communities. **e** Relative abundance of soil microorganisms at the phylum level. **f** Sterilization experiment

desorption in soil were first analyzed. The contact angle of NBC was 121.9°, whereas that of nZVI was 0°, indicating strong lipophilicity for NBC and pronounced hydrophilicity for nZVI (Fig. S9a). NBC and ZVI were uniformly dispersed in NC-ZVI through ball milling, imparting amphiphilic characteristics to the catalyst. The results showed that NC-ZVI was uniformly distributed throughout the entire water–oil (n-hexane) system, whereas bare ZVI was dispersed in the water phase (Fig. S9b). As a result, the amphiphilicity of NC-ZVI facilitated the mass transfer of acetochlor from the soil phase to NC-ZVI, thus promoting its desorption from the soil phase because of the strong binding affinity of NC-ZVI for acetochlor. Desorption experiments of acetochlor in soil indicated that NC-ZVI induced a desorption rate of 24.1% for acetochlor in soil (Fig. 4c), which was 9.2-fold and 22.7-fold greater than those of S-ZVI (2.61%) and nZVI (1.06%), respectively. These findings suggest that N/C doping significantly enhanced both the mass transfer dynamics and desorption rate of NC-ZVI toward soil acetochlor. This trend aligns with the adsorption capacity observed in aqueous-phase-acetochlor adsorption tests (Fig. S10), fully demonstrating that NC-ZVI has a stronger binding affinity for acetochlor compared with soil alone, which leads to the effective desorption of acetochlor from the soil. Consequently, the incorporation of N/C heteroatoms can greatly enhance the amphiphilicity of NC-ZVI and improve the binding affinity of ZVI, the soil desorption capacity, and the migration of acetochlor from soil to ZVI materials, thereby efficiently degrading acetochlor.

The composition of the microbial species of the harvested rhizosphere soil was analyzed to determine its role in acetochlor degradation. Principal coordinate analysis (PCoA) revealed that the bacterial community structures of acetochlor-contaminated soil samples treated with NC-ZVI and those exposed solely to acetochlor were distinctly separated (Fig. 4d), suggesting that NC-ZVI amendment significantly altered the bacterial community structure. Particularly, NC-ZVI shifted the soil microbial profile closer to that of the untreated group without acetochlor exposure, indicating at least partial restoration of the acetochlor-stressed microbial community to a healthier state (Fig. S11a). Furthermore, the abundance of *Bacteroidota*, a dominant dechlorinating phylum, significantly increased in response to NC-ZVI treatment during maize cultivation; its relative abundance increased by 14.6% compared to 10.6% in the acetochlor-only control group (Fig. 4e). Meanwhile, the known dehalogenating genus *Dehalogenimonas* was significantly enriched in all acetochlor-contaminated treatment groups. Its abundance increased from 0.4% in the control group without acetochlor to 1.1% in the acetochlor-only treatment group, and its relative abundance further increased to 1.8% after NC-ZVI addition, representing a 63.6% increase (Fig. S11b). Typical dechlorinating bacteria harboring multiple *rdh* genes, including *Dehalogenimonas lykanthroporepellens* and *Dehalogenimonas alkenigignens*, have been confirmed to participate in the dechlorination of organic pollutants (Molenda et al. 2016; Qiao et al. 2022). Therefore, it can be speculated that soil microorganisms play a crucial role in acetochlor detoxification. As anticipated, soil sterilization experiments quantified microbial contributions, revealing that soil microbiota mediated 12.6% of the total degradation of acetochlor, while the synergistic effect of NC-ZVI and microbes accounted for an additional 22.3% enhancement (Fig. 4f).

3.4 Root iron plaques as strong barriers against both acetochlor and its byproducts

Crop phytotoxicity and food safety risks from soil herbicide residue arise not only from the parent compound but also from its transformation products (Sandín-España et al. 2015). This study systematically investigated the dynamics of acetochlor and its degradation products (e.g., acetochlor OXA, acetochlor ESA, and CMEPA) in the soil-maize system. Unexpectedly, their concentrations in maize leaves treated with NC-ZVI (0.006 mg kg^{-1} and 0.003–0.01 mg kg^{-1}) were significantly lower than those in the acetochlor-contaminated group (0.08 mg kg^{-1} and 0.03–0.06 mg kg^{-1}). This suggests the presence of an active barrier mechanism for plant uptake of acetochlor and its degradation products, which operates beyond catalytic degradation within the soil–plant system. Previous studies have shown that root iron plaque can serve as a primary barrier against pollutant transfer from soil to plant roots (He et al. 2024; Yue et al. 2025). In this study, the detected concentration of acetochlor in NC-ZVI-mediated root iron plaque from the NC-ZVI treatment was 0.62 mg kg^{-1}, which was 3.4-fold higher than that in the acetochlor-contaminated group (0.18 mg kg^{-1}) (Fig. 5a). By contrast, the acetochlor concentration in maize roots treated with NC-ZVI accounted for only 8.6–21.2% of that in root iron plaque; similarly, the total concentrations of acetochlor degradation products in root iron plaque were significantly greater than those in maize roots (Fig. 5b, c; Fig. S12), indicating that root iron plaque acts as a primary reservoir for the accumulation of acetochlor and its degradation products. Leveraging this effect of iron plaque, NC-ZVI reduced the total concentration of both acetochlor and its degradation products in maize by 81.2% compared to the acetochlor-contaminated group.

SEM and TEM images further revealed a solid aggregate plaque on the surfaces of maize roots treated with

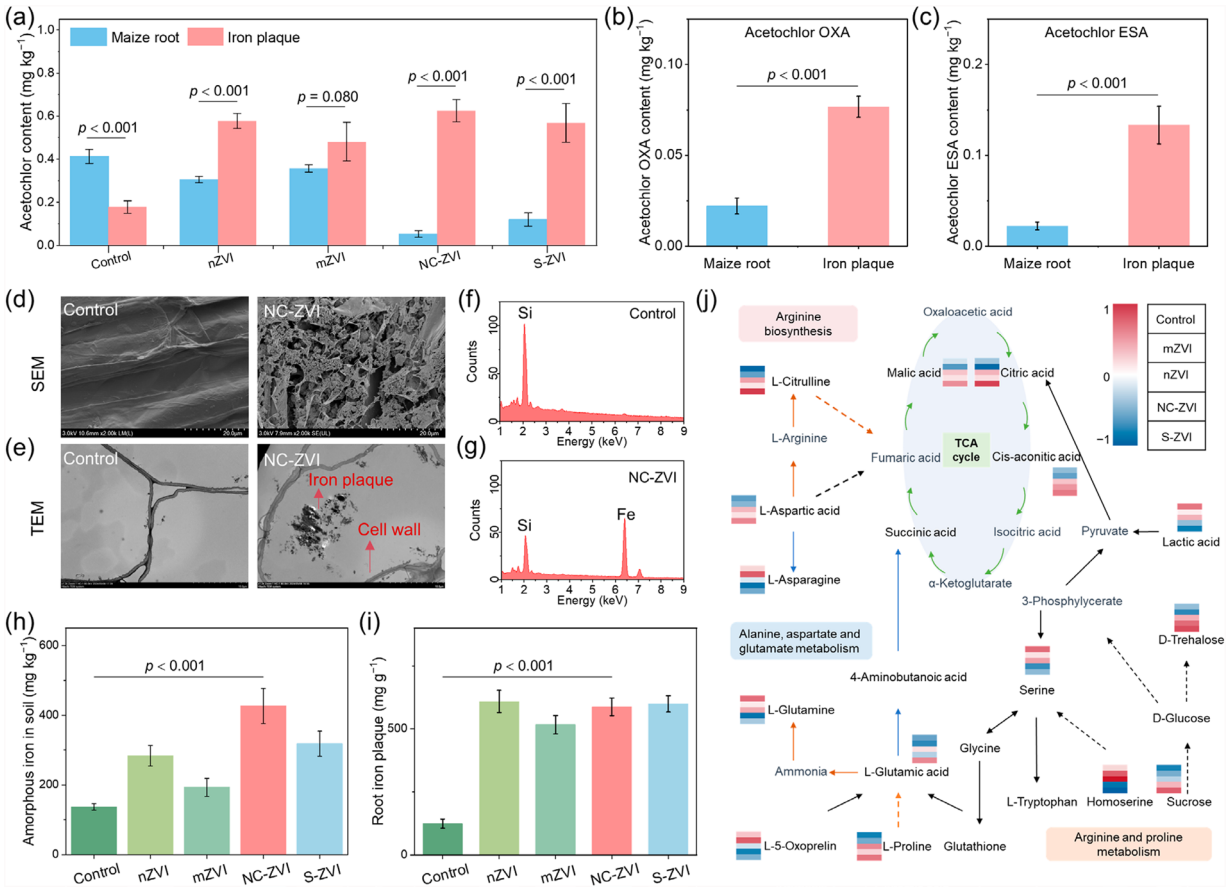

Fig. 5 Iron plaque formation and its barrier effect on pollutant transportation. **a** Acetochlor, (**b**) acetochlor OXA, and (**c**) acetochlor ESA content in maize root and iron plaque. **d** SEM images of the root surface. **e** TEM images of the intercellular space of roots exposed to NC-ZVI. TEM-EDS analysis for (**f**) Control and (**g**) NC-ZVI. **h** Amorphous iron content in soil. **i** Root iron plaque content. **j** Root metabolic pathway map

NC-ZVI. EDS images obtained from TEM confirmed that the aggregate plaque contained iron elements (Fig. 5d–g; Fig. S13). Consequently, it was inferred that NC-ZVI facilitated the formation of iron plaque on the maize root surface. Previous studies have shown that, in addition to sufficient iron supplementation, iron plaque formation may also be affected by soil iron species and root exudates, such as amorphous iron and acidic substances secreted by plant roots (Zheng et al. 2024). Therefore, we conducted a systematic analysis of soil physicochemical properties and root metabolites to further elucidate the mechanism underlying iron plaque formation. Our results revealed that the content of amorphous iron in the soil significantly increased in response to the ZVI materials compared with the acetochlor-contaminated group, with contents increasing from 137.0 mg kg^{-1} to 426.6 and 318.3 mg kg^{-1} for NC-ZVI and S-ZVI treatments, respectively (Fig. 5h). This increase in the amorphous iron content was attributed to iron supplementation from the added ZVI materials and the soil's weak acidic conditions (Fig. S14), which collectively created an environment conducive to iron plaque formation. As a result, the content of iron plaque under NC-ZVI treatment also significantly increased (Fig. 5i). Furthermore, the increase in organic acids, such as malic acid, citric acid, and cis-aconitic acid, within the root metabolic pathways provided additional evidence (Fig. 5j), as root acidic metabolites have been shown to increase the release of iron ions in the soil, thereby regulating iron plaque formation (Zheng et al. 2024). Additionally, maize plants were precultured in NC-ZVI-treated soil for 21 d and subsequently transplanted into acetochlor-contaminated soil for 14 d. The results indicated that after pre-cultivation with NC-ZVI, the acetochlor content in the iron plaque was higher than that in the acetochlor-only treatment, while the acetochlor content in maize leaves decreased by 73.3% (Fig. S15). These findings confirm that iron plaque serves as an effective barrier to reduce acetochlor uptake by maize.

Based on the above findings, we proposed a novel mechanism for the efficient remediation of acetochlor-contaminated soil using NC-ZVI. The N/C coordination imparts amphiphilic properties and high surface

reactivity to NC-ZVI, thereby enhancing its ability to adsorb and degrade acetochlor in soil. Furthermore, NC-ZVI synergizes with rhizosphere functional microorganisms to achieve efficient chemical and biological remediation of acetochlor-contaminated soil, achieving 96.7% removal for the herbicide acetochlor within 21 d. Meanwhile, NC-ZVI mediates the controlled release of iron ions, enhances the total iron ion concentration in soil, and stimulates the formation of iron plaque on the root surfaces of maize plants. This iron plaque effectively prevents the uptake of acetochlor and its byproducts by maize plants due to its strong adsorption and immobilization of organic pollutants. This multi-interface regulation not only synergistically ensures the effective remediation of herbicide-contaminated soil but also significantly reduces the uptake of herbicides and their degradation products by maize, thereby mitigating the adverse effects caused by herbicide soil pollution.

3.5 Ecological compatibility and techno-economic viability assessment of NC-ZVI

Soil microbiota play pivotal roles in ecosystem functions, including nutrient cycling and organic pollutant degradation (Philippot et al. 2024). Our results demonstrate that NC-ZVI restructured the microbial communities under acetochlor stress while preserving ecological functions. Further quantitative analysis revealed that acetochlor exposure reduced soil microbial diversity, with Chao1, Shannon, and Simpson indices decreasing by 2.66–9.63% relative to the uncontaminated control group (Fig. 6a; Fig. S16), indicating the ecotoxicity of acetochlor to soil microbes (Hao et al. 2018). Remarkably, the NC-ZVI amendment reversed these adverse effects, increasing the alpha diversity index by 5.6–15.0% compared to acetochlor-only treatments. Control experiments confirmed the ecological safety of NC-ZVI, showing no significant inhibition of microbial growth, consistent with the previously reported favorable environmental compatibility of biochar-ZVI material (Shen et al. 2025). These findings

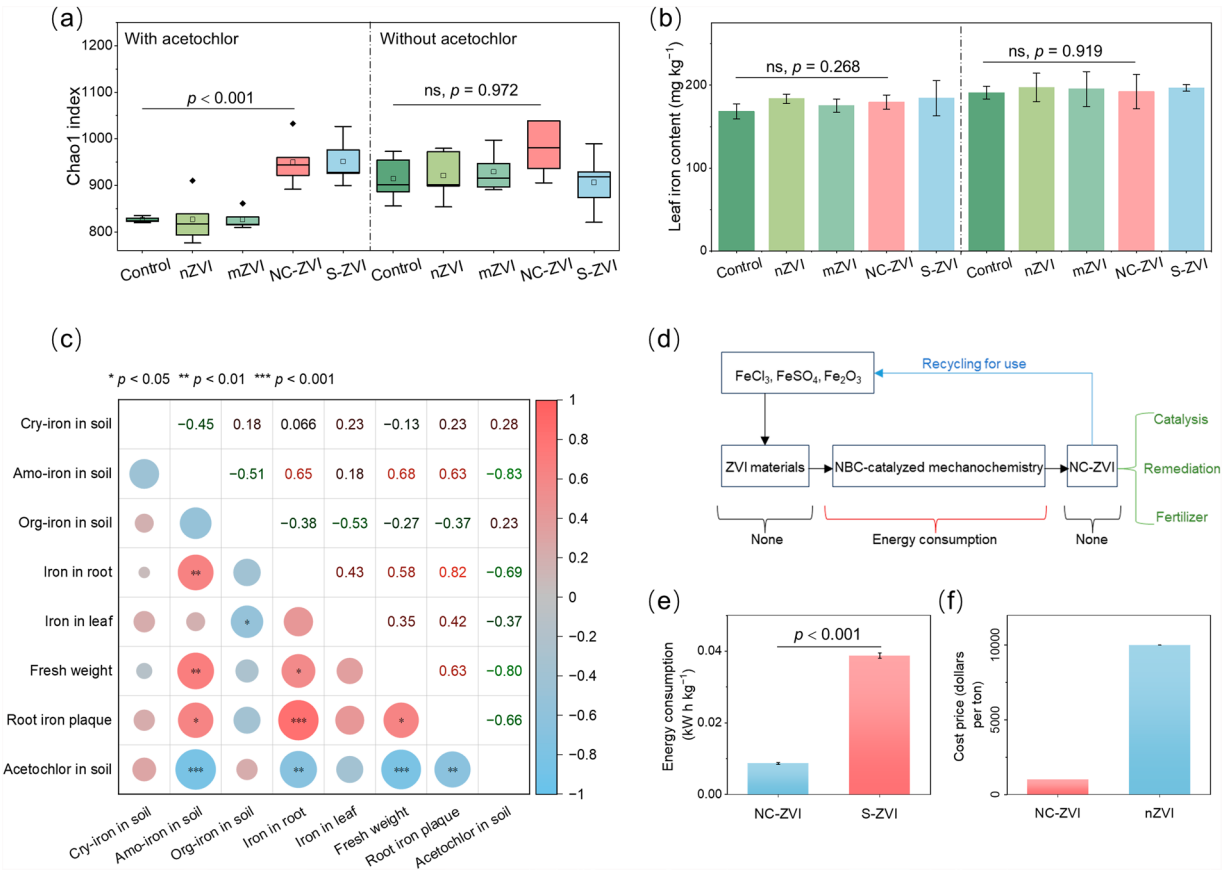

Fig. 6 Long-term application potential and environmental feasibility assessments. **a** Chao1 index of soil microbiota. **b** Maize leaf iron content. **c** Pearson correlation matrix of different iron contents and maize yields. The color from green to red represents the Pearson correlation coefficient from −1 to 1. **d** System boundary of NBC-catalyzed mechanochemistry synthesis of NC-ZVI. **e** Energy consumption for synthesizing NC-ZVI from 36 g of ZVI and 4 g of NBC as feedstock. **f** The cost price of preparing NC-ZVI and nZVI per ton. ns is not significant

establish NC-ZVI as both an effective remediation agent and an ecologically compatible amendment for herbicide-contaminated soils.

The environmental implications of NC-ZVI and its impact on iron uptake in crops were systematically evaluated. Although NC-ZVI treatment resulted in significant iron accumulation in maize roots, foliar iron levels remained unchanged, indicating restricted translocation (Fig. 6b). The iron in roots originates primarily from the adsorption of iron materials on root surfaces, with minimal uptake resulting from the internalization of iron particles and the absorption of ionized iron released from iron particles and other iron-containing minerals. This observation is consistent with previous reports showing root-cell internalization but no upward transport of nZVI in poplar and limited translocation of nZVI from root to aerial parts of cucumber (Dwivedi et al. 2018; Li et al. 2021a; Zhu et al. 2024). In this study, NC-ZVI exhibited no phytotoxicity while concurrently enhancing maize shoot weight and reducing maize uptake of acetochlor and its byproducts (Fig. 6c), thereby demonstrating its dual functionality as both an effective remediation agent and a source of iron nutrition. However, it should be noted that although limited transport reduces the risk of short-term phytotoxicity and dietary exposure, the long-term ecological effects of repeated application of NC-ZVI, such as the potential for iron accumulation in soil and its impacts on soil ecology and groundwater safety, still need to be further studied.

The energy consumption evaluation of NC-ZVI synthesis from a given biomass provides important insights for future production scale-up and sustainable applications. Figure 6d shows the theoretical boundaries involved in the mechanochemical synthesis of NC-ZVI. Therefore, the main energy process considered is the power consumption related to ball milling. As shown in Fig. 6e, the unit energy consumption of NC-ZVI was 77.6% lower than that of S-ZVI under the same process, which can be attributed to the increased ball milling efficiency resulting from the addition of NBC (Wang et al. 2024). According to the International Energy Agency, the carbon emission coefficient of electricity is approximately 0.5 kg CO_2 per kilowatt-hour (Shi et al. 2024). Consequently, from a quantitative perspective, optimizing NC-ZVI materials can efficiently enhance energy savings and reduce carbon emissions. This energy efficiency is essential for promoting low-carbon milling processes and achieving cost control. Notably, the cost of mZVI is considerably lower than that of nZVI (Wei et al. 2022a). Preliminary estimates indicate that the cost of NC-ZVI synthesized by ball milling is less than $1000 per ton (Fig. 6f), which is only one-tenth of the cost price of nZVI (more than $10,000 per ton). This cost advantage facilitates the large-scale manufacturing of NC-ZVI, thereby mitigating the impact of soil organic pollutants on crops in farmland. The promising laboratory-scale data warrant further investigation into scalable production strategies. Future efforts should focus on optimizing process parameters for industrial scale-up production, conducting a comprehensive life-cycle assessment to verify environmental benefits, and evaluating long-term field efficacy to fully ascertain the technology's practical potential and economic feasibility.

4 Conclusions

In summary, the novel NC-ZVI developed in this work achieved efficient remediation of herbicide contamination in soil–plant systems and safe crop production through multi-interface synergistic modulation. The Fe–C and Fe–N coordination, as well as N-doped active sites in NC-ZVI, reconstructed the electronic structure of ZVI, significantly enhanced its surface reaction activity and electron transfer efficiency, and strengthened the interfacial desorption and catalytic degradation of acetochlor in soil. The formation of the rhizosphere iron plaque barrier induced by NC-ZVI effectively prevented the maize uptake of acetochlor and its degradation products, thereby reducing dietary risks for maize. This synergistic strategy of "soil catalytic degradation-root iron plaque barrier" breaks through the bottleneck of traditional technologies that are difficult to balance the rapid removal of pollutants and crop safety. Meanwhile, the optimization of the material synthesis process further highlights the advantages of low energy consumption and low cost. These findings provide new insights and economical solutions for developing agricultural environmental remediation nanotechnologies, contributing to the sustainable development of the ecological environment and ensuring food security. However, the impact of NC-ZVI on iron nutrition and the yield of mature crops remains unclear. Therefore, future research could focus on the transformation of this material in agricultural environments and its long-term effects on crop yields in contaminated soils to promote its field application.

Supplementary Information

The online version contains supplementary material available at https://doi.org/10.1007/s42773-025-00567-8.

Additional file 1.

Author contributions

All authors contributed to the study conception and design. Xiangyu Zhang: Data curation, Methodology, Visualization, Writing-original draft. Peng Zhang: Funding acquisition, Writing review & editing. Le Jiao: Writing review & editing. Yanwei Zhang: Writing review & editing. Hongwen Sun: Supervision, Writing review & editing. Chenglan Liu: Funding acquisition, Resources,

Supervision, Writing review & editing. And all authors commented on previous versions of the manuscript.

Funding
This work was supported by the National Natural Science Foundation of China (U21A20291, 42577439), the National Key Research and Development Program of China (2021YFD1000500), and the 111 program, Ministry of Education of China (B17025).

Data availability
Data will be available upon reasonable request.

Declarations

Competing interests
Hongwen Sun is an EBM of the journal Biochar, and he was not involved in the peer-review or handling of the manuscript. The authors have no relevant financial or non-financial interests to disclose.

Author details
[1]National Key Laboratory of Green Pesticide, College of Plant Protection, South China Agricultural University, Guangzhou 510642, China. [2]MOE Key Laboratory of Pollution Processes and Environmental Criteria, College of Environmental Science and Engineering, Nankai University, Tianjin 300350, China. [3]Ministry of Agriculture and Rural Affairs, Agro-Environmental Protection Institute, Tianjin 300191, China.

Received: 23 July 2025 Revised: 10 December 2025 Accepted: 24 December 2025
Published online: 11 February 2026

References

Amaral DC, Lopes G, Guilherme LRG et al (2017) A new approach to sampling intact Fe plaque reveals Si-induced changes in Fe mineral composition and shoot As in rice. Environ Sci Technol 51(1):38–45. https://doi.org/10.1021/acs.est.6b03558

Arshad N, Alam S, Rafay M et al (2024) Effects of environmental relevant concentrations of acetochlor on growth, hematology, serum biochemistry and histopathology of Japanese quail. PLoS ONE 19(9):e0306583. https://doi.org/10.1371/journal.pone.0306583

Bokulich NA, Subramanian S, Faith JJ et al (2013) Quality-filtering vastly improves diversity estimates from Illumina amplicon sequencing. Nat Methods 10(1):57–59. https://doi.org/10.1038/nmeth.2276

Chen P, Zhou T, Xing L et al (2017) Atomically dispersed iron-nitrogen species as electrocatalysts for bifunctional oxygen evolution and reduction reactions. Angew Chem Int Ed 56(2):610–614. https://doi.org/10.1002/anie.201610119

Chen C, Zhou Q, Guo Z et al (2024) Lattice-sulfur-impregnated zero-valent iron crystals for long-term metal encapsulation. Nat Sustain 7(10):1264–1272. https://doi.org/10.1038/s41893-024-01409-4

Dwivedi AD, Yoon H, Singh JP et al (2018) Uptake, distribution, and transformation of zerovalent iron nanoparticles in the edible plant *Cucumis sativus*. Environ Sci Technol 52(17):10057–10066. https://doi.org/10.1021/acs.est.8b01960

Food and Agriculture Organization of the United Nations (2015) Status of the World's Soil Resources. https://www.fao.org/family-farming/detail/en/c/357394/

Gao J, Wang W, Rondinone AJ et al (2015) Degradation of trichloroethene with a novel ball milled Fe–C nanocomposite. J Hazard Mater 300:443–450. https://doi.org/10.1016/j.jhazmat.2015.07.038

Gong L, Qiu X, Tratnyek PG et al (2021) FeN_X(C)-coated microscale zero-valent iron for fast and stable trichloroethylene dechlorination in both acidic and basic pH conditions. Environ Sci Technol 55(8):5393–5402

Gong L, Chen J, Zhan G et al (2025) Mechanochemical molten-salt-assisted surface nitridation promotes electron transfer dechlorination of zerovalent iron. Environ Sci Technol 59(19):9802–9811

González-Curbelo MÁ, Socas-Rodríguez B, Herrera-Herrera AV et al (2015) Evolution and applications of the QuEChERS method. TrAC Trends Anal Chem 71:169–185. https://doi.org/10.1016/j.trac.2015.04.012

Grillet L, Lan P, Li W et al (2018) IRON MAN is a ubiquitous family of peptides that control iron transport in plants. Nat Plants. https://doi.org/10.1038/s41477-018-0266-y

Gu Y, Wang B, He F et al (2017) Mechanochemically sulfidated microscale zero valent iron: pathways, kinetics, mechanism, and efficiency of trichloroethylene dechlorination. Environ Sci Technol 51(21):12653–12662

Guan X, Chen X, Qiu C et al (2020) Effects of long-term herbicide application on the crops in soybean-peanut rotations in the red soil upland of Southern China. Field Crops Res 248:107723. https://doi.org/10.1016/j.fcr.2020.107723

Han C, Liu Z, Teng Y et al (2025) Careful attention to the eco-toxicity and secondary water pollution of the degradation by-products. Environ Res 271:121091. https://doi.org/10.1016/j.envres.2025.121091

Hao Y, Zhao L, Sun Y et al (2018) Enhancement effect of earthworm (*Eisenia fetida*) on acetochlor biodegradation in soil and possible mechanisms. Environ Pollut 242:728–737. https://doi.org/10.1016/j.envpol.2018.07.029

He Z, Chen J, Yuan S et al (2024) Iron plaque: a shield against soil contamination and key to sustainable agriculture. Plants 13(11):1476. https://doi.org/10.3390/plants13111476

Herrick JE, Fowler C, Sibanda LM et al (2024) The vision for adapted crops and soils: how to prioritize investments to achieve sustainable nutrition for all. Nat Plants 10(12):1840–1846. https://doi.org/10.1038/s41477-024-01867-w

Hoang TT, Qi C, Paul KC et al (2021) Epigenome-wide DNA methylation and pesticide use in the Agricultural Lung Health Study. Environ Health Perspect 129(9):097008. https://doi.org/10.1289/EHP8928

Huang P, Zhang P, Wang C et al (2022) Enhancement of persulfate activation by Fe-biochar composites: synergism of Fe and N-doped biochar. Appl Catal B 303:120926. https://doi.org/10.1016/j.apcatb.2021.120926

Leng X, Zhao L, Gao S et al (2023) Review on the discovery of novel natural herbicide safeners. J Agric Food Chem 71(30):11320–11331. https://doi.org/10.1021/acs.jafc.3c03585

Li Y, Liu X, Wu X et al (2018) Effects of biochars on the fate of acetochlor in soil and on its uptake in maize seedling. Environ Pollut 241:710–719. https://doi.org/10.1016/j.envpol.2018.05.079

Li M, Zhang P, Adeel M et al (2021a) Physiological impacts of zero valent iron, Fe_3O_4 and Fe_2O_3 nanoparticles in rice plants and their potential as Fe fertilizers. Environ Pollut 269:116134. https://doi.org/10.1016/j.envpol.2020.116134

Li Y, Zhao HP, Zhu L (2021b) Remediation of soil contaminated with organic compounds by nanoscale zero-valent iron: a review. Sci Total Environ 760:143413. https://doi.org/10.1016/j.scitotenv.2020.143413

Li X, Zhang X, Zhang P et al (2023) Incorporation of N-doped biochar into zero-valent iron for efficient reductive degradation of neonicotinoids: mechanism and performance. Biochar 5(1):78. https://doi.org/10.1007/s42773-023-00280-4

Li Y, Zhang J, Xu L et al (2025) Leaf absorption contributes to accumulation of microplastics in plants. Nature 641(8063):666–673. https://doi.org/10.1038/s41586-025-08831-4

Lin L, Zhu Q, Xu AW (2014) Noble-Metal-Free Fe-N/C catalyst for highly efficient oxygen reduction reaction under both alkaline and acidic conditions. J Am Chem Soc 136(31):11027–11033. https://doi.org/10.1021/ja504696r

Liu Y, Wu T, White JC et al (2021) A new strategy using nanoscale zero-valent iron to simultaneously promote remediation and safe crop production in contaminated soil. Nat Nanotechnol 16(2):197–205. https://doi.org/10.1038/s41565-020-00803-1

Liu Y, Wang Y, Wu T et al (2022) Synergistic effect of soil organic matter and nanoscale zero-valent iron on biodechlorination. Environ Sci Technol 56(8):4915–4925. https://doi.org/10.1021/acs.est.1c05986

Meng FL, Zhang X, Hu Y et al (2024) New barrier role of iron plaque: producing interfacial hydroxyl radicals to degrade rhizosphere pollutants. Environ Sci Technol 58(1):795–804. https://doi.org/10.1021/acs.est.3c08132

Molenda O, Quaile AT, Edwards EA (2016) *Dehalogenimonas* sp. strain WBC-2 genome and identification of its *trans*-dichloroethene reductive dehalogenase. TdrA. Appl Environ Microbiol 82(1):40–50. https://doi.org/10.1128/AEM.02017-15

Philippot L, Chenu C, Kappler A et al (2024) The interplay between microbial communities and soil properties. Nat Rev Microbiol 22(4):226–239. https://doi.org/10.1038/s41579-023-00980-5

Qiao W, Liu G, Li M et al (2022) Complete reductive dechlorination of 4-hydroxy-chlorothalonil by *Dehalogenimonas* populations. Environ Sci Technol 56(17):12237–12246. https://doi.org/10.1021/acs.est.2c02574

Qu J, Li Z, Bi F et al (2023) A multiple Kirkendall strategy for converting nano-sized zero-valent iron to highly active Fenton-like catalyst for organics degradation. Proc Natl Acad Sci USA 120(39):e2304552120. https://doi.org/10.1073/pnas.2304552120

Radwan DEM (2012) Salicylic acid induced alleviation of oxidative stress caused by clethodim in maize (*Zea mays* L.) leaves. Pestic Biochem Physiol 102(2):182–188. https://doi.org/10.1016/j.pestbp.2012.01.002

Reuschenbach P, Silvani M, Dammann M et al (2008) ECOSAR model performance with a large test set of industrial chemicals. Chemosphere 71:1986–1995. https://doi.org/10.1016/j.chemosphere.2007.12.006

Sandín-España P, Sevilla-Morán B, Villarroya-Ferruz M et al (2015) Comparative phytotoxicity assays of the herbicide Alloxydim and its main identified photoproduct in cereal and broadleaves crops. Weed Sci 63(2):377–387. https://doi.org/10.1614/WS-D-14-00122.1

Shen L, Cai Y, Gao J (2025) Effects of nanoscale zero-valent iron loaded biochar on the fate of phenanthrene in soil-radish (*Raphanus sativus* L. var. radculus pers) system. Eco-Environment and Health 4(1):100134. https://doi.org/10.1016/j.eehl.2025.100134

Shi Y, Li L, Zhou W et al (2024) Regulating the surface area increase of zero-valent iron (ZVI) during ball milling: a study of the mechanical mechanism and low-carbon milling. Powder Technol 446:120177. https://doi.org/10.1016/j.powtec.2024.120177

Tang FHM, Lenzen M, McBratney A et al (2021) Risk of pesticide pollution at the global scale. Nat Geosci 14(4):206–210. https://doi.org/10.1038/s41561-021-00712-5

Umeh AC, Duan L, Naidu R et al (2017) Residual hydrophobic organic contaminants in soil: are they a barrier to risk-based approaches for managing contaminated land? Environ Int 98:18–34. https://doi.org/10.1016/j.envint.2016.09.025

Wang D, Lin H, Ma Q et al (2021a) Manganese oxides in *Phragmites* rhizosphere accelerates ammonia oxidation in constructed wetlands. Water Res 205:117688. https://doi.org/10.1016/j.watres.2021.117688

Wang Y, Guo H, Gao X et al (2021b) The intratumor microbiota signatures associate with subtype, tumor stage, and survival status of esophageal carcinoma. Front Oncol 11:754788. https://doi.org/10.3389/fonc.2021.754788

Wang W, Li M, Diao L et al (2023) The health risk of acetochlor metabolite CMEPA is associated with lipid accumulation induced liver injury. Environ Pollut 331:121857. https://doi.org/10.1016/j.envpol.2023.121857

Wang X, Huang P, Zhang P et al (2024) Incorporation of N-doped biochar into submicron zero-valent iron for efficient peroxydisulfate activation in soil remediation: performance and mechanism. Chem Eng J 482:148832. https://doi.org/10.1016/j.cej.2024.148832

Wang X, Zhang P, Wang W et al (2025) New insights into the role of crystalline Fe_3P in phosphatized zerovalent iron for enhancing advanced oxidation processes and storage stability. Environ Sci Technol 59(12):6319–6330. https://doi.org/10.1021/acs.est.4c14797

Wei K, Li H, Gu H et al (2022a) Strained zero-valent iron for highly efficient heavy metal removal. Adv Funct Mater 32(26):2200498. https://doi.org/10.1002/adfm.202200498

Wei L, Zhu Z, Razavi BS et al (2022b) Visualization and quantification of carbon "rusty sink" by rice root iron plaque: mechanisms, functions, and global implications. Glob Change Biol 28(22):6711–6727. https://doi.org/10.1111/gcb.16372

Xie W, Zhu A, Ali T et al (2023) Crop switching can enhance environmental sustainability and farmer incomes in China. Nature 616(7956):300–305. https://doi.org/10.1038/s41586-023-05799-x

Xie W, Peng C, Chen A et al (2024) Synergistic adsorption and degradation of sulfonylurea herbicides by biochar-supported nano zero-valent iron composites in in-situ soil remediation. Chem Eng J 500:156927. https://doi.org/10.1016/j.cej.2024.156927

Xu N, Zhang X, Guo P et al (2024) Biological self-protection inspired engineering of nanomaterials to construct a robust bio-nano system for environmental applications. Sci Adv 10(38):eadp2179. https://doi.org/10.1126/sciadv.adp2179

Yan P, Du Q, Chen H et al (2023) Biofortification of iron content by regulating a NAC transcription factor in maize. Science 382(6675):1159–1165. https://doi.org/10.1126/science.adf3256

Yue J, Hu X, Xie H et al (2025) Enhancing emerging pollutant removal mediated by root iron plaques: integrated abiotic and biotic effects. J Hazard Mater 485:136900. https://doi.org/10.1016/j.jhazmat.2024.136900

Zeller AK, Zeller YI, Gerhards R (2021) A long-term study of crop rotations, herbicide strategies and tillage practices: effects on *Alopecurus myosuroides* Huds. abundance and contribution margins of the cropping systems. Crop Prot 145:105613. https://doi.org/10.1016/j.cropro.2021.105613

Zhang K, Li W, Li H et al (2023) A leaf-patchable reflectance meter for in situ continuous monitoring of chlorophyll content. Adv Sci 10(35):2305552. https://doi.org/10.1002/advs.202305552

Zhao F, Li Y, Duan X et al (2025) Optimal farm size reduces global poverty-induced soil antibiotic exposure risk. Nat Food 6(4):353–364. https://doi.org/10.1038/s43016-025-01131-0

Zheng T, Hou J, Wu T et al (2024) Ferric oxide nanomaterials and plant-rhizobacteria symbionts cogenerate iron plaque for removing highly chlorinated contaminants in dryland soils. Environ Sci Technol 58(25):11063–11073. https://doi.org/10.1021/acs.est.4c03133

Zhu S, Chen M, Dai H et al (2024) Safe production of rice in Cd-polluted paddy fields by rhizosphere application of zero-valent iron nanoplates at specific growth stages. Nano Today 56:102289. https://doi.org/10.1016/j.nantod.2024.102289